

Hydrogen in Laves phase ZrX_2 ($X=V, Cr, Mn, Fe, Co, Ni$) compounds: Binding energies and electronic and magnetic structure

Suklyun Hong^{1,2,*} and C. L. Fu¹¹*Metals and Ceramics Division, Oak Ridge National Laboratory, Oak Ridge, Tennessee 37831-6114*²*Department of Physics, Sejong University, Kwangjin, Seoul 143-747, Korea*

(Received 12 December 2002; published 18 September 2002)

The effects of hydrogen on the ground-state electronic and magnetic structures of AB_2 ($A=Zr$; $B=V, Cr, Mn, Fe, Co, Ni$) Laves phase compounds were investigated by first-principles local-density-functional calculations. We calculated the relative stability of atomic hydrogen at various interstitial tetrahedral sites formed by two A atoms and two B atoms ($2A2B$ site), one A atom and three B atoms ($1A3B$ site), and four B atoms ($4B$ site). We find that (i) for ZrV_2 and $ZrCr_2$, hydrogen prefers the site with the largest interstitial hole size (i.e., $2A2B$ site); (ii) for $ZrMn_2$, $ZrFe_2$, and $ZrCo_2$, the hydrogen binding energies at the $1A3B$ site become comparable to or even lower than those at the $2A2B$ site once the antibonding states of B atoms become progressively occupied. In H-free $ZrFe_2$, we found a large magnetic moment ($0.5\mu_B$) at the Zr site, which is coupled antiparallel to the moment at the Fe site ($1.9\mu_B$). The hydrogen absorption does not have a strong effect in suppressing the magnetic moments of atoms closest to the absorbed hydrogen but increases the magnetic moments of atoms not having hydrogen as the nearest neighbor. This increase in the moment is partly due to the H-induced lattice expansion.

DOI: 10.1103/PhysRevB.66.094109

PACS number(s): 71.20.Lp

I. INTRODUCTION

Hydrogen storage materials are usually intermetallics containing interstices with a suitable binding energy for hydrogen which allows its absorption or desorption near room temperature and atmospheric pressure. A promising candidate for hydrogen storage is the class of Laves phase compounds having the formula unit AB_2 .¹ Laves phase includes the fcc C15 ($MgCu_2$), hexagonal C14 ($MgZn_2$), and dihedral C36 ($MgNi_2$) structures. They transform from one to the other during heating and cooling (typically C14 at high temperatures and C15 at low temperatures). The C15 structure is a fcc-based structure containing six atoms (two formula units) in the primitive unit cell, while the C14 and C36 structures are hexagonal structures containing 12 and 24 atoms in the primitive unit cell, respectively.

The interstitial sites occupied by hydrogen in AB_2 Laves phases are tetrahedral sites formed by two A atoms and two B atoms ($2A2B$ site) or by one A atom and three B atoms ($1A3B$ site) or four B atoms ($4B$ site). There are 17 tetrahedral interstitial sites per formula unit:² 12 $2A2B$ sites, four $1A3B$ sites, and one $4B$ site for both the C15 and C14 structures. In the C15 structure, A or B atoms within each type of sites ($2A2B$, $1A3B$, and $4B$) are locally equivalent. This is not the case for the C14 structure. Depending on the local environment of the tetrahedra, the 12 $2A2B$ sites and four $1A3B$ sites per formula unit in the C14 structure can be further grouped into six $2A2B(l)$ sites, three $2A2B(k_2)$ sites, 1.5 $2A2B(h_2)$ sites, 1.5 $2A2B(h_1)$ sites, one $1A3B(f)$ site, and three $1A3B(k_1)$ sites.² To depict the interstitial sites formed by A and/or B atoms, a ball-stick model of the face-centered cubic (fcc) C15 structure is given in Fig. 1. The $2A2B$ site has the largest interstitial hole size and the $4B$ site has the smallest.

In this paper, the binding energy and site preference of hydrogen in ZrX_2 ($X=V, Cr, Mn, Fe, Co, Ni$) are studied by first-principles local-density-functional calculations. These results allow us to investigate the correlation between electronic structure and hydrogen binding in ZrX_2 -based compounds. The magnitude of the binding energy at these interstitial sites is an important factor to consider in addressing the hydrogen storage capacity.

The effect of hydrogen on the magnetic properties of ZrX_2 is also an intriguing subject. Hydrogen absorption was reported to increase the magnetic moments and magnetic ordering temperature in $Zr(Fe,Cr)_2$ and $ZrMn_2$.³ Thus the effects of hydrogen on the magnetic moments of $ZrFe_2$ and

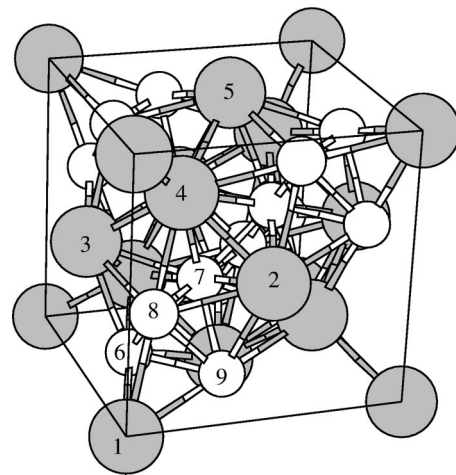


FIG. 1. The C15 Laves phase structure, where the larger and the smaller atoms represent A (Zr) and B ($X=V, Cr, Mn, Fe, Co, Ni$), respectively. Here, for example, a $2A2B$ site is formed by the atoms labeled 2, 4, 7, and 8; a $1A3B$ site by atoms 1, 6, 8, and 9; and a $4B$ site by atoms 6, 7, 8, and 9.

TABLE I. The experimental lattice constants (a_{expt}) and the binding energies (E_B) of hydrogen in ZrX_2 (i.e., $\text{ZrX}_2\text{H}_{0.5}$) in units of kJ/mol H.

X	a_{expt}	$E_B(2A2B)$	$E_B(1A3B)$	$E_B(4B)$	E_B^{expt}
V	7.448	-83.0	-75.1	-29.8	-77 ~ -80 [9]
Cr	7.208	-33.5	-25.2	-1.4	-19[10] ~ -23 [9]
Mn (C15)	7.135	-24.2	-24.8	-8.2	
Fe	7.074	-5.8	-6.6	0.4	
Co	6.951	-8.9	-16.0	-4.3	
Ni	6.925	3.3	15.2	36.2	

ZrMn_2 were also investigated. We found that the absorbed hydrogen atoms do not have a strong effect in suppressing the magnetic moments of Fe or Mn. On the other hand, there is an increase in the averaged magnetic moment away from the H-absorption sites, partly due to the H-induced lattice expansion. In a H-free ZrFe_2 compound, we obtained a large magnetic moment ($0.5\mu_B$) on the Zr site, which is coupled antiparallel to the moment at the Fe site. The calculated magnetic moments for H-free ZrFe_2 agree well with previous theoretical^{4,5} and experimental⁶ works.

II. METHODOLOGY AND APPROACH

Total-energy calculations of Zr-based alloys have been performed using the full-potential linearized augmented plane-wave (FLAPW) method⁷ within the local-density approximation (LDA) with the Hedin-Lundqvist exchange-correlation potential. The FLAPW method solves the local-density-functional equations without any shape approximation to the potential or charge density. We use the fcc primitive unit cell containing two formula units for the calculation of a H-containing C15 structure, and the hcp unit cell having four formula units for C14. The muffin-tin radius (r_{mt}) of 2.15 a.u. is used for Cr, Mn, Fe, and Co, and $r_{mt} = 2.30$ a.u., 2.05 a.u., and 2.85 a.u. are used for V, Ni, and Zr, respectively. The kinetic-energy cutoff of 24 Ry for the charge density expansion and a $6 \times 6 \times 6$ k -mesh in the Monkhorst special k -point scheme are used. The calculations are scalar relativistic. We use 70–90 plane waves per atom for the expansion of wave functions. The self-consistency is reached when the root-mean-square distance between the input and output charge densities is less than 0.1 me/(a.u.)³. The atomic positions are relaxed by calculating Hellmann-Feynman forces acting on the atoms. The convergence criterion for the force is 0.003 Hartree/(a.u.).

To study the effects of hydrogen in ZrX_2 , we considered a system containing one atomic hydrogen in the C15 fcc primitive cell. The formula of the system is $\text{ZrX}_2\text{H}_{0.5}$. The hydrogen absorption induces an increase in the size of the unit cell without changing the structure. The experimentally observed volume expansion is about 2.9 \AA^3 per hydrogen atom. This expansion corresponds to about 1% increase in the lattice constant for $\text{ZrX}_2\text{H}_{0.5}$. In this investigation we are interested in the relative stability of hydrogen in different tetrahedral sites for a given compound as well as in the general trend in the site preference of hydrogen as the atomic number of X

increases. In this regard, due to the small change in the energies with $\sim 1\%$ change in the lattice parameter, we assume that $\text{ZrX}_2\text{H}_{0.5}$ has the same lattice parameter as ZrX_2 in calculating the hydrogen binding energies for a low hydrogen concentration. It should also be noted that, since the local-density-functional approximation underestimates the lattice constants of these ZrX_2 compounds by 3–4%, we used the experimental lattice constants for a better description of the interstitial hole size in the calculation of hydrogen binding energies. However, for magnetic systems (ZrMn_2 and ZrFe_2), because of the sensitivity of the size of the magnetic moments to the volume, we have additionally considered the effect of lattice expansion (due to the presence of hydrogen) in addressing the magnetic properties of these compounds using the generalized gradient approximation¹⁴(GGA) for the exchange-correlation potential. Specially, the PBE-type functional¹⁴ is adopted in the GGA approach, and a kinetic-energy cutoff of 40 Ry and a $10 \times 10 \times 10$ k -mesh are used in the calculations using the GGA.

Other than the C14 structure of ZrMn_2 , all the other binary ZrX_2 alloys studied here have the C15 structure. In order to have a meaningful comparison of the dependence of hydrogen binding energy on the number of valence electrons in these compounds, we first assumed ZrMn_2 to have the hypothetical C15 structure. At the end, we then calculated the hydrogen binding energy at selected interstitial sites in C14 ZrMn_2 to examine the variation of hydrogen binding energy with respect to structure. The formula of the C14 system used in our calculation is $\text{ZrMn}_2\text{H}_{0.25}$.

III. RESULTS AND DISCUSSION

A. Hydrogen binding energies in ZrX_2 compounds

The binding energy of hydrogen is defined by

$$E_B = \frac{1}{n} \left[E(AB_2H_n) - E(AB_2) - \frac{n}{2} E(H_2) \right] \quad (1)$$

where $E(H_2)$, $E(AB_2)$, and $E(AB_2H_n)$ are the energies of H_2 , AB_2 , and AB_2 with n hydrogen atoms per formula unit, respectively. Here, we used $E(H_2)$ as sum of the energy of two widely separate hydrogen atoms and the dissociation energy of H_2 (432 kJ/mol H_2), as given by experiment.⁸

The results for the hydrogen binding energy are shown in Table I (also see Fig. 2). Note that 1 kJ/mol H = 1.0364×10^{-2} eV/H. From the calculations, ZrMn_2 and ZrFe_2 are

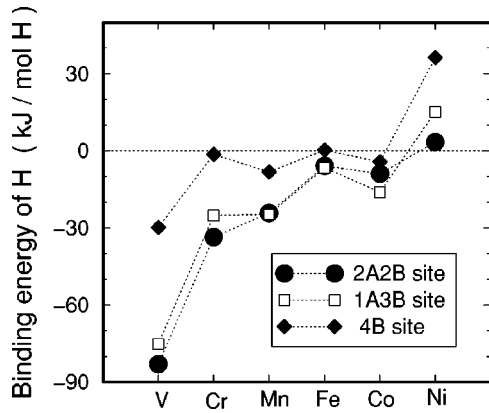


FIG. 2. Binding energy of hydrogen in C15 ZrX_2 ($X=V, Cr, Mn, Fe, Co, Ni$).

the only magnetic systems among these ZrX_2 compounds. The hydrogen binding energies in $ZrMn_2$ and $ZrFe_2$ are obtained from the spin-polarized states.

In general, in these ZrX_2 compounds, the absolute value of the hydrogen binding energy decreases as the atomic number of X increases; eventually, the atomic hydrogen atoms become unstable in $ZrNi_2$. The site preference of absorbed hydrogen also shows an interesting behavior. For ZrV_2 and $ZrCr_2$, hydrogen at the 2A2B site has the lowest binding (most stable) energy, as expected from the largest interstitial hole size formed by the 2A2B tetrahedra. On the other hand, for $ZrMn_2$ (with the hypothetical C15 structure), $ZrFe_2$ and $ZrCo_2$, the hydrogen binding energies at the 1A3B site become comparable to or even lower than those at the 2A2B site as the antibonding states of X are progressively filled. The possible explanation for this trend will be discussed in Sec. III B. It is interesting to note that, as the electronic states become more localized in $ZrNi_2$, the interstitial hole size, again, is the dominant factor in determining the relative stability of hydrogen in various sites (i.e., the 2A2B site is the least unstable). The calculated hydrogen binding energies of 2A2B and/or 1A3B for ZrV_2 and $ZrCr_2$ show good agreement with experiment: the measured values are $-77 \sim -80$ kJ/mol H for ZrV_2 and $-19 \sim -23$ kJ/mol H for $ZrCr_2$.^{9,10}

B. Electronic structure of ZrX_2 and $ZrX_2H_{0.5}$

First we consider the electronic density of states (DOS) of ZrV_2 and $ZrCr_2$, which are shown in Figs. 3 and 4, respectively. In general, the DOS profile exhibits a well-defined valley separating the bonding and antibonding states. For ZrV_2 , the Fermi energy lies in the vicinity of bonding states with the DOS at the Fermi level, $N(E_F)$, ~ 6.4 states/eV spin. This value is smaller than previous theoretical ones.^{11,12} With hydrogen absorption ($ZrV_2H_{0.5}$), there is a slight downward shift of the DOS profile with respect to the Fermi energy, which results in a lower $N(E_F)$ by about 20% (see the inset of Fig. 3). The downward shift of the DOS is expected to be more pronounced with more hydrogen present in ZrV_2 , which has been observed in $ZrV_2H_{1.3}$ [the experimentally estimated $N(E_F)$ is about 2.7 states/eV spin].¹³ For

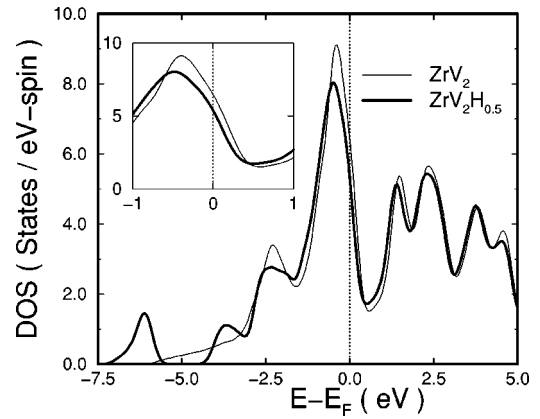


FIG. 3. Total density of states of ZrV_2 and $ZrV_2H_{0.5}$.

the case of $ZrCr_2$, the Fermi level is at the bonding-antibonding valley of the DOS profile, as shown in Fig. 4. There is no noticeable change in $N(E_F)$ after hydrogen absorption. The lowering of $N(E_F)$ for $ZrV_2H_{0.5}$ as compared to ZrV_2 may partly account for the strong binding of hydrogen in ZrV_2 .

From both chemical (i.e., electronegativity) and geometrical (i.e., interstitial hole size) points of view, atomic hydrogen would prefer 2A2B (i.e., 2Zr2X) sites in these ZrX_2 compounds, since Zr forms a more stable hydride with the 2A2B site being the largest interstitial hole. Results of our calculation, however, show different trends in the site preference of hydrogen in these ZrX_2 compounds. While the 2A2B site offers the strongest binding for hydrogen in ZrV_2 and $ZrCr_2$, hydrogen at the 1A3B site becomes comparable and/or even lower in energy than at the 2A2B site for $ZrMn_2$, $ZrFe_2$, and $ZrCo_2$. Clearly, the electronic structure factor plays an important role in determining the site preference and binding energy of hydrogen. Our calculations show that hydrogen is strongly bound in ZrV_2 , and becomes weakly bound in $ZrFe_2$. The Zr-based Laves phases for hydrogen storage are, therefore, mostly based on $ZrCr_2$ and $ZrMn_2$ with hydrogen having a suitable binding energy in those compounds.

Analysis of the electronic structure shows that an isolated interstitial hydrogen in these ZrX_2 compounds is in the nega-

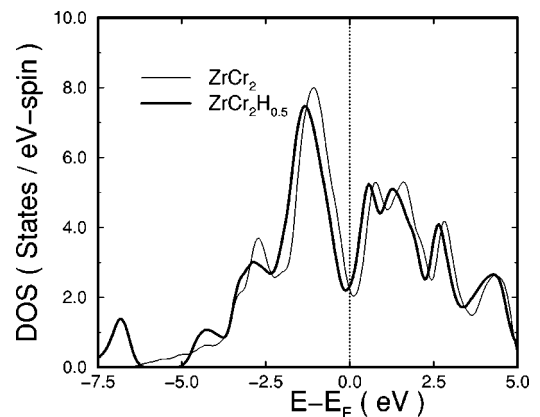


FIG. 4. Total density of states of $ZrCr_2$ and $ZrCr_2H_{0.5}$.

TABLE II. Magnetic moments (in units of μ_B) of Fe (Mn) and Zr in $ZrFe_2$ ($ZrMn_2$) and $ZrFe_2H_{0.5}$ ($ZrMn_2H_{0.5}$). The results at both the LDA and GGA levels are shown together for the $ZrFe_2$ case. The magnetic moments on the Fe (Mn) atoms closest to the absorbed hydrogen are underlined. The number of equivalent atoms is shown in the square brackets.

	Fe (LDA)	Zr (LDA)	Fe (GGA)	Zr(GGA)
H-free	1.80 [4]	-0.43 [2]	1.88 [4]	-0.51 [2]
with H at 1Zr3Fe site	1.96 [1], <u>1.59</u> [3]	<u>-0.39</u> [1], -0.41 [1]	2.07 [1], <u>1.69</u> [3]	<u>-0.45</u> [1], -0.47 [1]
with H at 2Zr2Fe site	1.98 [1], 1.88 [1], <u>1.61</u> [2]	<u>-0.37</u> [1], <u>-0.37</u> [1]	-	-
	Mn (LDA)	Zr (LDA)		
H-free	0.89 [4]	-0.22 [2]		
with H at 1Zr3Mn site	1.65 [1], <u>0.99</u> [3]	<u>-0.25</u> [1], -0.27 [1]		
with H at 2Zr2Mn site	1.54 [1], 1.69 [1], <u>0.67</u> [2]	<u>-0.24</u> [1], <u>-0.23</u> [1]		

tive charge state due to charge donation from host to hydrogen. The negative charge compels hydrogen to maximize its interatomic distance to the host atoms. Therefore, absorbed hydrogen generally prefers open interstitial sites. This is one of the reasons why hydrogen prefers $2A2B$ sites in ZrV_2 and $ZrCr_2$. On the other hand, as the atomic number of X increases in these ZrX_2 compounds, the antibonding d -states of the host X become progressively filled. Consequently, the depletion of the antibonding electrons through charge-transfer to hydrogen becomes a competitive bonding mode in the compounds with a higher number of valence electrons. The reason why hydrogen at the $1A3B$ site is more energetically favorable in $ZrMn_2$, $ZrFe_2$, and $ZrCo_2$ (although the $1A3B$ site has a smaller interstitial hole size than the $2A2B$ site) is due to the fact that the depletion of antibonding electrons by hydrogen is more likely to be accomplished by having more X atoms as the nearest neighbor of hydrogen.

Often, in order to have optimal hydrogen binding energy, the concept of electronegativity is used in designing the hydrogen storage materials. While this is a useful approach, our calculation clearly shows that this empirical guideline fails in many aspects. First, as mentioned already, it does not provide the correct site preference for hydrogen: The relative binding energy of hydrogen at different tetrahedra is an important factor to consider, since higher hydrogen capacity is more likely to be achieved if the hydrogen binding energies at the $2A2B$ and $1A3B$ sites are about equal. Second, it fails to predict the strong binding energy of hydrogen in ZrV_2 : The strong binding of hydrogen in ZrV_2 is due to the reduction of the electronic density of states at the Fermi level upon hydrogen absorption. Third, it is inadequate to describe the effect of magnetism in compounds based on Mn and Fe. We therefore believe that, in order to have a better control on the hydrogen storage properties of alloys, empirical guidelines such as electronegativity and atomic size are inadequate.

C. Magnetic properties of $ZrFe_2$ and $ZrMn_2$

In this section, we discuss the ground-state magnetic properties of $ZrFe_2$ and $ZrMn_2$ with and without interstitial hydrogen atoms. For H-containing compounds, we consider systems with one hydrogen atom in the C15 fcc primitive cell (i.e., $ZrFe_2H_{0.5}$ and $ZrMn_2H_{0.5}$) or in the C14 hexagonal primitive cell (i.e., $ZrMn_2H_{0.25}$). First, we calculated the

magnetic moments in the H-free compounds at the experimental lattice constant using the local-density-functional approach; the same approach was also used to calculate the magnetic moments of H-containing compounds at an 1% expansion in the lattice parameter (by following the empirical rule) for the C15 structure. For a better (and more precise) description of the interplay between structural and magnetic properties, we later used the GGA approach¹⁴ to minimize the total energies with respect to lattice parameter in both the H-free and H-containing $ZrFe_2$. The GGA approach yields a lattice constant in better agreement with the experiment (than the LDA approach) for H-free compounds. The lattice constant of $ZrFe_2$ by the GGA approach is about 0.7% less than the experimental value. Furthermore, the GGA approach finds a lattice expansion of 1.2% for $ZrFe_2H_{0.5}$, which agrees well with the value derived from the empirical rule. For the magnetic moments, the GGA and LDA approaches basically give the same results in both trend and magnitude. The GGA results listed in Table II are the magnetic moments at the equilibrium lattice constants.

First, we consider the $ZrFe_2$ case. The calculation shows that sizable magnetic moments are on both Zr and Fe sites. We note that Zr has a large magnetic moment ($0.5\mu_B$), which is coupled antiparallel to the moment at the Fe site ($1.9\mu_B$). These calculated results are in good agreement with previous calculations: (i) $1.90\mu_B$ at the Fe site and $-0.56\mu_B$ at the Zr site⁴, and (ii) $1.86\mu_B$ at the Fe site and $-0.61\mu_B$ at the Zr site.⁵ Also, our results compare well with the neutron diffraction studies, which give $2.11\mu_B$ ($1.90\mu_B$) at the Fe site and $-0.32\mu_B$ ($-0.34\mu_B$) at the Zr site, where the numbers in parentheses were obtained by considering a diffuse magnetization.⁶ Similarly to the case of Fe-V alloys,¹⁵ our analysis shows that the hybridization between Zr and Fe has a larger effect through the minority-spin channel than the majority-spin channel. This is evidenced in well-defined bonding and antibonding hybrids in the minority-spin DOS profile with the Fermi energy located at the valley separating these two hybrids (see Fig. 5).

In the H-free C15 structure, all four Fe atoms in the primitive cell are equivalent. In the case of hydrogen at the interstitial site, the Fe atoms are divided into nonequivalent types. In Table II, we only cite the magnetic moments for hydrogen

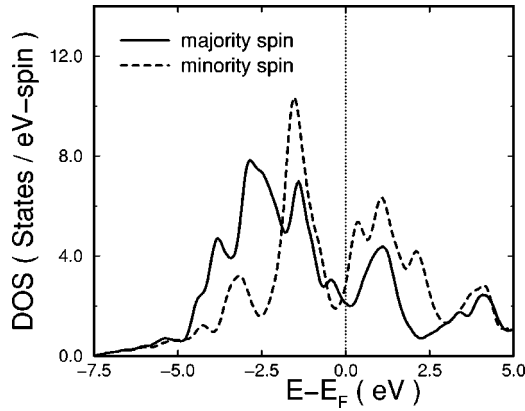


FIG. 5. Density of states of majority and minority spins of $ZrFe_2$ using the equilibrium lattice constant at the GGA level.

at the lowest energy configurations (i.e., at the $1Zr3Fe$ and $2Zr2Fe$ sites); the values of the magnetic moments of Fe and Zr closest to hydrogen are underlined. It should be noted that these are the results for hydrogen atoms forming an ordered fcc lattice. Since the magnetic structure induced by defects or interstitials can have long-range effects, the values of the magnetic moments may depend on the arrangement of hydrogen atoms in the lattice. Nevertheless, the basic trend in the effect of hydrogen on magnetic moments can be obtained from our model calculations.

In general, the effect of absorbed hydrogen is to decrease the magnetic moments of Fe having hydrogen as the nearest neighbor by $\sim 0.2\mu_B$, but to increase the magnetic moments of Fe farther away from hydrogen by an amount $\sim (0.1-0.2)\mu_B$. On the other hand, the effect of hydrogen on the magnetic moments of Zr is comparatively small. Note that there is a difference in the lattice parameters by $\sim 1\%$ with and without hydrogen. The reduction in the moments is obviously due to the hybridization between hydrogen and its nearest-neighbor Fe atoms. To examine the effect of lattice expansion, we have also calculated the magnetic moments of H-containing compounds without including the 1% expansion in lattice parameter. We found that the 1% increase in the lattice parameter increases nearly uniformly the magnetic moments of all Fe atoms by $(0.1-0.2)\mu_B$. In other words, the increase in the magnetic moment due to hydrogen absorption mainly comes from the H-induced lattice expansion in the case of $ZrFe_2$.

For $ZrMn_2$ in either the hypothetical C15 structure or the C14 structure, the magnetic moments are smaller than those of $ZrFe_2$. In H-free C15 $ZrMn_2$, the Mn atom has a moment of $0.89\mu_B$ and is coupled antiparallel to the moment of Zr ($0.22\mu_B$). When hydrogen atoms are absorbed at the $1Zr3Mn$ and $2Zr2Mn$ sites, the change in the magnetic moments of Mn atoms closest to hydrogen is relatively small as compared to the sizeable increase in the moments of Mn atoms farther away from hydrogen (see Table II). Part of the increase ($\sim 0.2\mu_B$) is again attributed to the effect of H-induced lattice expansion. It is unclear, however, if the majority of the increase is due to the artifact of an ordered fcc structure used in the calculation for H-absorbed sites. We note that, from $ZrMn_2$ to $ZrFe_2$, the number of the minority-

spin electrons remains almost the same; the change in the number of electrons is basically from the majority-spin channel. This leads to a higher density-of-states at E_F for the majority-spin channel of $ZrMn_2$ than that of $ZrFe_2$, and may explain why the spin-density of $ZrMn_2$ is more sensitive to the perturbation in the environment.

In H-free C14 $ZrMn_2$, there are two nonequivalent types of Mn atoms with moments $0.62\mu_B$ (with six equivalent atoms/cell) and $1.03\mu_B$ (with two equivalent atoms/cell), respectively. Experimentally, it has been observed that the magnetic susceptibility of H-free $ZrMn_2$ increases with decreasing temperature;³ thus we cannot rule out the possibility of a magnetic ground state of $ZrMn_2$, as found theoretically.

In the C14 structure, since there are many nonequivalent interstitial sites (within the classes of $2A2B$ and $1A3B$ sites) available for hydrogen absorption, the calculation on the effect of hydrogen requires a careful sampling of various H-absorption sites and their arrangements. We have considered a few (limited) cases by including a hydrogen atom in the primitive cell of the C14 structure, i.e., $ZrMn_2H_{0.25}$. For those sites with higher weights (in terms of the numbers of sites available), we found that the binding energies of hydrogen at the $2Zr2Mn$ and $1Zr3Mn$ sites are nearly equal and are within ~ 5 kJ/mol of those in the C15 $ZrMn_2$, i.e., the binding energies are -30.3 , -26.0 , and -28.1 kJ/mol for the $2A2B(k_2)$, $2A2B(l)$, and $1A3B(k_1)$ sites, respectively. This finding is not unexpected, considering that the difference in the C14 and C15 structures comes from the layer stacking sequences. A similar trend (as in the case of C15 structure) is also found in the H-induced change in the magnetic moments, although the hydrogen atoms form a different lattice (i.e., hexagonal lattice) in this case. The trend includes a slight change (by $\sim 0.1\mu_B$) in the magnetic moment of Mn atoms closest to hydrogen and the H-induced oscillations in the magnitudes of moments away from the H-absorption sites. The averaged moment away from the H-absorption sites is found to increase. For the $2A2B(k_2)$ site, the largest increase (by $0.7\mu_B$) comes from the moments of Mn atoms that are the second-nearest-neighbor (2nd-nn) of absorbed hydrogen. For the $1A3B(k_1)$ site, the magnetic moment of the 2nd-nn Mn also has the largest increase (by $0.5\mu_B$). For the $2A2B(l)$ site, the magnetic moment of the 2nd-nn Mn increases by $0.35\mu_B$.

IV. SUMMARY

The binding energy and site preference of hydrogen in ZrX_2 ($X=V, Cr, Mn, Fe, Co, Ni$) Laves phase compounds were investigated by a first-principles LDA approach. The absolute value of the hydrogen binding energy decreases as the atomic number of X increases, and eventually the hydrogen becomes unstable in $ZrNi_2$. For early transition metals, hydrogen atoms prefer an interstitial site with the largest interstitial hole size. For middle and late transition metals, the depleting of antibonding states of X (due to host-to-H charge transfer) appears to be a competitive bonding mode in determining the site preference of hydrogen atoms.

The ground state of $ZrMn_2$ and $ZrFe_2$ is magnetic. The

large magnetic moment is found for Zr, which is coupled antiparallel to the magnetic moments of Fe and Mn. It is clear from our calculations that the absorbed hydrogen (in the low concentration limit) does not cause a significant reduction in the magnetic moments of its nearest neighbor Fe or Mn atoms. On the other hand, the effect of H-induced lattice expansion partially account for the increase in the magnetic moments of Fe and Mn atoms away from the H-absorption sites; the amount of increase is about $0.2\mu_B$ per 1% expansion in the lattice parameter for both Fe and Mn atoms.

ACKNOWLEDGMENTS

The work was sponsored by the Division of Materials Sciences and Engineering, Office of Basic Energy Sciences. Oak Ridge National Laboratory is operated by UT-Battelle, LLC, for the U.S. Department of Energy under Contract No. DE-AC05-00OR22725. This research was also supported in part by an appointment to the U.S. Department of Energy Higher Education Research Experience Program for Faculty at the Oak Ridge National Laboratory administered by the Oak Ridge Institute for Science and Education.

*Electronic address: hong@sejong.ac.kr

- ¹D. Shaltiel, *J. Less-Common Met.* **73**, 329 (1980), See the references therein.
- ²D.P. Shoemaker, and C.B. Shoemaker, *J. Less-Common Met.* **68**, 43 (1979).
- ³I. Jacob, D. Davidov, and D. Shaltiel, *J. Magn. Magn. Mater.* **20**, 226 (1980).
- ⁴P. Mohn and K. Schwarz, *Physica B&C* **130B**, 26 (1985).
- ⁵S. Asano and S. Ishida, *J. Magn. Magn. Mater.* **70**, 187 (1987).
- ⁶P. Warren, J.B. Forsyth, G.J. McIntyre, and N. Bernhoeft, *J. Phys.: Condens. Matter* **4**, 5795 (1992), and references therein.
- ⁷E. Wimmer, H. Krakauer, M. Weinert, and A.J. Freeman, *Phys. Rev. B* **24**, 864 (1981).
- ⁸P.W. Atkins, *Molecular Quantum Mechanics*, 2nd ed. (Oxford

University Press, Oxford, 1983), p. 257.

- ⁹A. Pebler and E.A. Gulbransen, *Trans. Metall. Soc. AIME* **239**, 1593 (1967).
- ¹⁰A.T. Pedziwiatr, R.S. Craig, W.E. Wallace, and F. Pourarian, *J. Solid State Chem.* **46**, 336 (1983).
- ¹¹B.M. Klein, W.E. Pickett, D.A. Papaconstantopoulos, and L.L. Boyer, *Phys. Rev. B* **27**, 6721 (1983).
- ¹²T. Jarlborg and A.J. Freeman, *Phys. Rev. B* **22**, 2332 (1980).
- ¹³C. Geibel, W. Goldacker, H. Keiber, V. Oestreich, H. Rietschel, and H. Wühl, *Phys. Rev. B* **30**, 6363 (1984).
- ¹⁴J.P. Perdew, K. Burke, and M. Ernzerhof, *Phys. Rev. Lett.* **77**, 3865 (1996).
- ¹⁵D.D. Johnson, F.J. Pinski, and J.B. Staunton, *J. Appl. Phys.* **61**, 3715 (1987).